Aalborg Universitet

AALBORG UNIVERSITY
DENMARK

Coupled-Mode Flutter of Wind Turbines and its Suppression Using Torsional Viscous Damper

Zhang, Zili; Chen, Bei; Nielsen, Søren R. K.

Published in:
Procedia Engineering

DOI (link to publication from Publisher):
10.1016/j.proeng.2017.09.352

Publication date:
2017

Document Version
Accepted author manuscript, peer reviewed version

Link to publication from Aalborg University

Citation for published version (APA):
Zhang, Z., Chen, B., & Nielsen, S. R. K. (2017). Coupled-Mode Flutter of Wind Turbines and its Suppression Using Torsional Viscous Damper. Procedia Engineering, 199, 3254–3259. DOI: 10.1016/j.proeng.2017.09.352

General rights
Copyright and moral rights for the publications made accessible in the public portal are retained by the authors and/or other copyright owners and it is a condition of accessing publications that users recognise and abide by the legal requirements associated with these rights.

? Users may download and print one copy of any publication from the public portal for the purpose of private study or research.
? You may not further distribute the material or use it for any profit-making activity or commercial gain
? You may freely distribute the URL identifying the publication in the public portal ?

Take down policy
If you believe that this document breaches copyright please contact us at vbn@aub.aau.dk providing details, and we will remove access to the work immediately and investigate your claim.

Downloaded from vbn.aau.dk on: August 15, 2018

Available online at www.sciencedirect.com

SciVerse ScienceDirect

Procedia Engineering 00 (2017) 000–000

Procedia Engineering

www.elsevier.com/locate/procedia

X International Conference on Structural Dynamics, EURODYN 2017

Coupled-Mode Flutter of Wind Turbines and its Suppression Using Torsional Viscous Damper

Zili Zhang[a,*], Bei Chen[b], Søren R.K. Nielsen[c]

[a]*Department of Engineering, Aarhus University, 8000 Aarhus, Denmark*
[b]*Key Laboratory for Wind and Bridge Engineering, Hunan University, 410082 Changsha, China*
[c]*Department of Civil Engineering, Aalborg University, 9000 Aalborg, Denmark*

Abstract

The trend towards lighter and more flexible blades may lead to aeroelastic instability of wind turbines under certain circumstances, resulting in rapid destructive failure or limit-cycle oscillations of the structural components. For pitch-regulated wind turbines, classical flutter is believed to become an increasingly important design consideration as blades become longer and slender. Flutter is an aeroelastic instability phenomenon where a torsional blade mode couples to a flap-wise bending mode, leading to a mutual rapid growth of the amplitude of the flap-wise and torsional motions. In this paper, a detailed finite element (FE) model for the wind turbine system is developed, with consistent modeling of the coupling between aerodynamic, elastic and inertial loads which have significant influence on the coupled-mode (flap-wise and torsional) vibration and stability. Further, elastic coupling between blade vibrations with tower and drivetrain motions are also considered, making this model capable for coupled-mode flutter analysis of a complete wind turbine system. The parameters of the model have been calibrated to the DTU 10MW wind turbine, and the critical flutter speed of the rotor is shown to be about 1.6 times its nominal rotational speed. A novel torsional viscous damper is then proposed to suppress torsional blade vibration and to enhance flutter stability of wind turbines.
© 2017 The Authors. Published by Elsevier Ltd.
Peer-review under responsibility of the organizing committee of EURODYN 2017.

Keywords: wind turbines, flutter, FE model, torsional viscous damper

1. Introduction

With the increasing size, future wind turbine designs will likely be stability-driven in contrast to the current loads-driven designs [1]. Modern pitch regulated variable-speed wind turbines normally do not operate in stall, and the risk of stall-induced vibration is not as serious as for stall-regulated wind turbines [2]. On the other hand, although classical flutter has not been observed on modern pitch-regulated wind turbines yet, it is believed to become a very important design consideration as wind turbine blades become longer and more flexible [2,3]. As the length of the wind turbine blades increases with the increasing rated capacity, the critical rotational speed for flutter will eventually approach the nominal rotational speed of the rotor, resulting in smaller stability margins for flutter [3,4]. Furthermore, blade

* Corresponding author. Tel.: +4593508334
E-mail address: zili_zhang@eng.au.dk

1877-7058 © 2017 The Authors. Published by Elsevier Ltd.
Peer-review under responsibility of the organizing committee of EURODYN 2017.

structural bend-twist coupling (BTC) has been proposed recently, as a way to passively mitigate the wind-induced fluctuating loads and to prolong the fatigue life [5]. Higher structural BTC is desirable to make fatigue load reduction, but it may also increase the risk of classical flutter due to the coupling of blade bending and torsional modes.

Comparing with stall-induced vibrations, flutter is a more violent aeroelastic instability where the first torsional blade mode couples to a flap-wise bending mode through the aerodynamic loads. Flutter takes place if the change of angle of attack due to the torsional deformation changes the lift force in an unfavorable phase with the flap-wise response. A wind turbine may have the risk of flutter when these conditions are met : 1) attached flow around the blade; 2) sufficiently high relative speed of the flow (sufficiently high rotational speed of the rotor) to ensure sufficient energy input; 3) eigenfrequencies of a flap-wise mode and the first torsional mode close to each other; 4) the mass center of gravity of the blade cross-section lies aft of the aerodynamic center [2]. Therefore, coupled-mode flutter becomes possible for large pitch-regulated wind turbines when the rotational speed of the rotor is large. It is of great importance to carry out accurate flutter analysis of a wind turbine system, in order to determine the critical rotational speed of the rotor for the onset of flutter (critical flutter speed) and to reveal the stability margin of the turbine.

In this paper, a rigorous finite element (FE) model for the wind turbine system has been developed, based on which flutter analysis of wind turbines is carried out. Unlike the widely-used 2D blade section model [4] for flutter analysis, the proposed FE model (3D) takes into account all important characteristics of a real wind turbine, e.g., the offsets between the center of gravity, the shear center and the aerodynamic center of each cross-section along the blade, the distribution of pre-twist along the blade, couplings between the blade vibrations with tower and drivetrain vibrations. All these effects are important for accurately carrying out flutter analysis and predicting the critical flutter speed. The DTU 10 MW wind turbine [6] has been used to calibrate the parameters of the FE model. Simulation results show that the critical flutter speed is about 1.6 times the nominal rotor rotational speed. Furthermore, a novel electromagnetic torsional viscous damper is proposed to be installed inside the blade, in order to damp the torsional vibration of the blade and to improve the flutter stability of the wind turbine system.

2. FE model of the aeroelastic wind turbine system

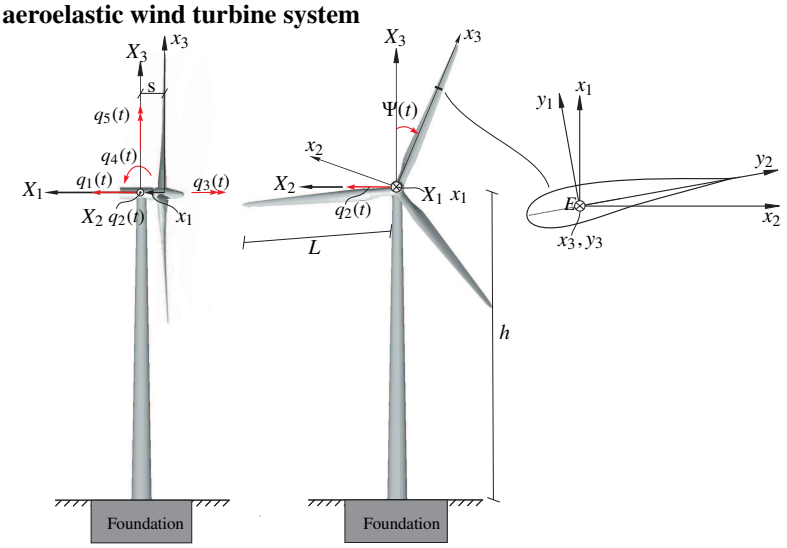

Fig. 1. Definition of different coordinate systems and the global degrees of freedom $q_1(t), \ldots, q_5(t)$.

A structural dynamic model for the complete wind turbine system is established. The tower and drivetrain are modeled with highly reduced number of degree-of-freedom (DOF), and each blade is modeled by detailed FE beam model. The coupled blade-tower -drivetrain vibrations are well accounted for.

2.1. Definition of three coordinate systems and the global DOFs

To accurately model the wind turbine, three different coordinate system are introduced as shown in Fig. 1. (X_1, X_2, X_3)-is the fixed, global coordinate system with its fixed origin O at the center of the tower top when the tower is unde-

formed. (x_1, x_2, x_3)- is the rotating blade coordinate system with its origin O' attached at the center of the hub. $\Psi(t)$ is the azimuthal angle of each rotating blade. Further, for each cross-section along the blade, a local principal axes coordinate system (y_1, y_2, y_3)- is introduced with origin at the bending center E of the cross-section. y_1-, y_2- are the two principal axes of the cross-section, and y_3- is co-directional to x_3- axis. L indicates blade length, h indicates the height of the tower from base, s is the horizontal distance between the center of the tower top and the center of hub.

The tower and drivetrain motions are modeled in the (X_1, X_2, X_3)- global coordinate system. A 5-DOF reduced order Bernoulli-Euler beam model is used for describing the tower motion [7,8], where $q_1(t)$ and $q_2(t)$ are the two translational DOFs, and $q_3(t)$, $q_4(t)$ and $q_5(t)$ are the three rotational DOFs (Fig. 1). The drivetrain is modeled by St. Venant torsional theory with 2-DOF $q_6(t)$ and $q_7(t)$ (not shown here), where $q_6(t)$ indicates elastic torsional deformation of the low speed shaft and $q_7(t)$ indicates elastic torsional deformation of the high speed shaft [7,8].

2.2. FE modeling of the rotating blade

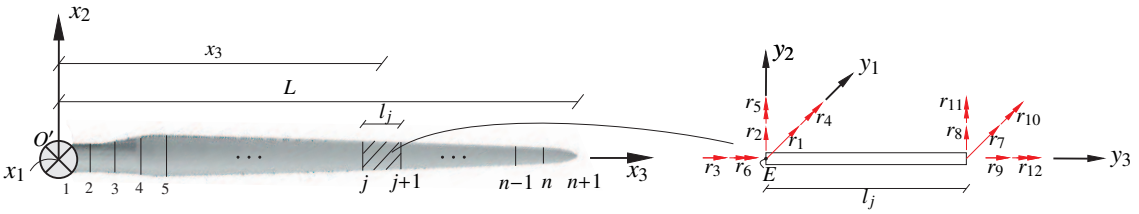

Fig. 2. Nodal numbering and definition of DOFs of a beam element.

Each blade is modeled as a Bernoulli-Euler beam in the rotating (x_1, x_2, x_3)- coordinate system. As shown in Fig. 2, the blade with the length L is discretized into n finite elements along the x_3- axis. For each element j, the principal axes coordinate system (y_1, y_2, y_3)- is introduced with origin at the bending center E of the cross-section. Let $\mathbf{r}(t) = [r_1, r_2, ..., r_{12}]^{\mathrm{T}}$ be a column vector storing the DOFs of the element j in the (y_1, y_2, y_3)- coordinate system. $\mathbf{u}^E(x_3, t) = [u_1^E, u_2^E, u_3^E, \theta_3^E]^{\mathrm{T}}$ denotes the elastic deformation field of the bending center E within the element, which can be obtained by the following interpolation:

$$\mathbf{u}^E(x_3, t) = \mathbf{N}^E(x_3)\mathbf{r}(t) \tag{1}$$

$\mathbf{N}^E(x_3)$ is a matrix containing related shape functions, from Bernoulli-Euler beam or St. Venant torsional theory.

Next, the deformation field of the center of gravity G within the element is expressed in terms of the DOFs $\mathbf{r}(t) = [r_1, r_2, ..., r_{12}]^{\mathrm{T}}$. As shown in Fig. 3, the following transformation between the deformation field of E and G holds:

$$\mathbf{u}^G(x_3, t) = \mathbf{A}(x_3)\mathbf{u}^E(x_3, t) \tag{2}$$

where $\mathbf{u}^G(x_3, t) = [u_1^G, u_2^G, u_3^G, \theta_3^G]^{\mathrm{T}}$. $\mathbf{A}(x_3)$ is the transformation matrix containing the offsets y_1^G and y_2^G of G from E. Therefore, $\mathbf{u}^G(x_3, t)$ can be written in terms of $\mathbf{r}(t)$:

$$\mathbf{u}^G(x_3, t) = \Big(\mathbf{A}(x_3)\mathbf{N}^E(x_3)\Big)\mathbf{r}(t) = \mathbf{N}^G(x_3)\mathbf{r}(t) \tag{3}$$

Furthermore, for each element j, the transformation between the blade coordinate system (x_1, x_2, x_3)- and the principal axes coordinate system (y_1, y_2, y_3)- is:

$$\mathbf{R}(t) = \mathbf{P}(x_3)\mathbf{r}(t) \tag{4}$$

where $\mathbf{R}(t) = [R_1, R_2, ..., R_{12}]^{\mathrm{T}}$ is a column vector storing the DOFs of the element j in the blade (x_1, x_2, x_3)- coordinate system. $\mathbf{P}(x_3)$ is the transformation matrix containing θ_j, the angle between x_1- axis and y_1- axis, as shown in Fig. 3a. Finally, the deformation field of the center of gravity G within the element is expressed in terms of the DOFs $\mathbf{R}(t)$:

$$\mathbf{u}^G(x_3, t) = \Big(\mathbf{N}^G(x_3)\mathbf{P}(x_3)\Big)\mathbf{R}(t) \tag{5}$$

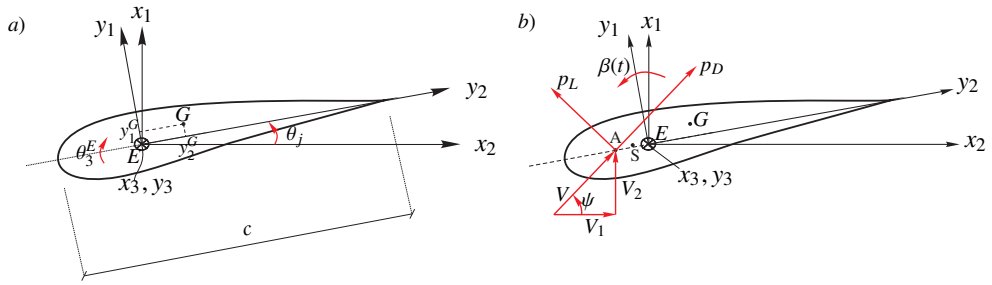

Fig. 3. Cross-section of the blade and two coordinate systems. a) Transfer of the deformation field from E to G. b) Aerodynamic loads acting on the aerodynamic center A.

The translational velocity vector of a cross-section of the rotating blade including the contributions from tower and drivetrain vibrations, in the moving (x_1, x_2, x_3)- coordinate system, can be written as [8]:

$$\mathbf{v}(x_3,t) = \begin{bmatrix} \dot{u}_1^G(x_3,t) + \dot{q}_1(t) + x_3\Big(\dot{q}_4(t)\cos\Psi + \dot{q}_5(t)\sin\Psi\Big) \\ \dot{u}_2^G(x_3,t) - \Omega u_3^G(x_3,t) + \dot{q}_2(t)\cos\Psi + s\Big(\dot{q}_4(t)\sin\Psi - \dot{q}_5(t)\cos\Psi\Big) - x_3\Big(\Omega + \dot{q}_6(t)\Big) \\ \dot{u}_3^G(x_3,t) + \Omega u_2^G(x_3,t) - \dot{q}_2(t)\sin\Psi + s\Big(\dot{q}_4(t)\cos\Psi + \dot{q}_5(t)\sin\Psi\Big) \end{bmatrix} \tag{6}$$

where $\Psi(t)$ is the azimuthal angle of the blade, and Ω is the rotational speed of the rotor.

The kinetic energy of each element can be obtained from the three translational velocities as well as the rotational velocity $\dot{\theta}_3^G$. From this kinetic energy, all the element mass matrices can be derived, such as the consistent mass matrix in conventional FE model, the mass matrices accounting for the coupling effect from tower and drivetrain. Then, the corresponding mass matrices of the whole blade can be obtained by assembling the element matrices.

2.3. Equations of motion of the wind turbine system

The above procedure is applied to all three blades. The total kinetic energy also includes that of the tower and of the drivetrain. The total potential energy can be easily calculated from all DOFs of the system. The equations of motion of the wind turbine system follow by inserting the kinetic and potential energies into the Lagrange equation:

$$\mathbf{M}(t)\ddot{\mathbf{Q}}(t) + \mathbf{C}(t)\dot{\mathbf{Q}}(t) + \mathbf{K}(t)\mathbf{Q}(t) = \mathbf{f}(\mathbf{Q},\dot{\mathbf{Q}},\beta(t),t) \tag{7}$$

where $\mathbf{M}(t)$, $\mathbf{C}(t)$ and $\mathbf{K}(t)$ are the time-dependent mass, damping, stiffness matrices. $\mathbf{Q}(t) = [\mathbf{Q}_0, \mathbf{R}_1, \mathbf{R}_2, \mathbf{R}_3]^{\mathrm{T}}$ is the column vector storing all DOFs of the system, where $\mathbf{Q}_0 = [q_1, q_2, ..., q_7]^{\mathrm{T}}$, $\mathbf{R}_1$, $\mathbf{R}_2$ and $\mathbf{R}_3$ store all DOFs of each of the three blades. The aerodynamic force vector $\mathbf{f}(\mathbf{Q},\dot{\mathbf{Q}},\beta(t),t)$ is calculated based on the classical blade element momentum (BEM) method [8,9], taking the quasi-static aeroelasticity, the pitch control angle $\beta(t)$ into consideration (Fig. 3b). It should be noted that in formulating $\mathbf{f}$, the lift force p_L and drag force p_D acting on the aerodynamic center A have been transferred to the shear center S.

3. Electromagnetic torsional viscous damper

Fig. 4 illustrates the proposed electromagnetic torsional viscous damper, which is installed inside the blade (inner part). It is well-known that when a conductive material is subjected to a time-varying magnetic flux, eddy currents are generated in the conductor. These eddy currents circulate inside the conductor, generating a magnetic field of opposite polarity as the applied magnetic field [11]. The interaction of the two magnetic fields induces a torque that resists the change in magnetic flux. This torque is proportional to the slip $\dot{r}_{6,j} - \dot{r}_{6,i}$, i.e., the difference between the angular velocities of the adjacent shafts, corresponding to a linear viscous damper with the damping constant c_t. The value of c_t can be easily changed by adjusting the magnetic field, making semi-active control possible.

The torsional damper is mainly composed with the magnetic bar and the conducting tube. The magnetic bar is attached to the inner shaft which is fixed close to the nacelle. The conducting tube is attached to the transmission shaft, the outer end of which is fixed at the mid board of blade (distance b from the inner fixed end).

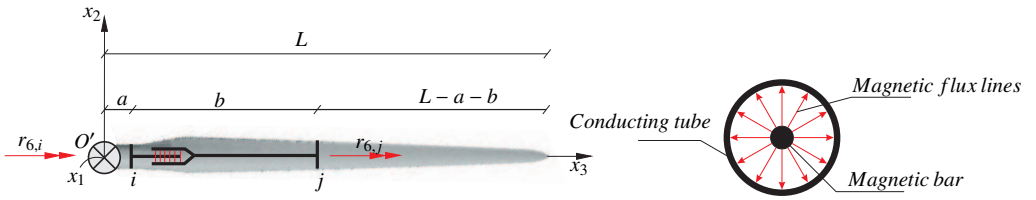

Fig. 4. The electromagnetic torsional viscous damper.

4. Simulation results

Data from DTU 10 MW wind turbine [6] have been used to calibrate the structural model of the wind turbine system. Each blade with a length 89 m is discretized into 50 elements, and the total number of DOFs of the system becomes $50 \times 6 \times 3+7=907$. A frozen isotropic and homogeneous turbulence filed is modelled by a vector ARMA model [10]. The rotational sampled turbulence is then obtained by converting the frozen field with a mean wind velocity V_0 into the rotating rotor.

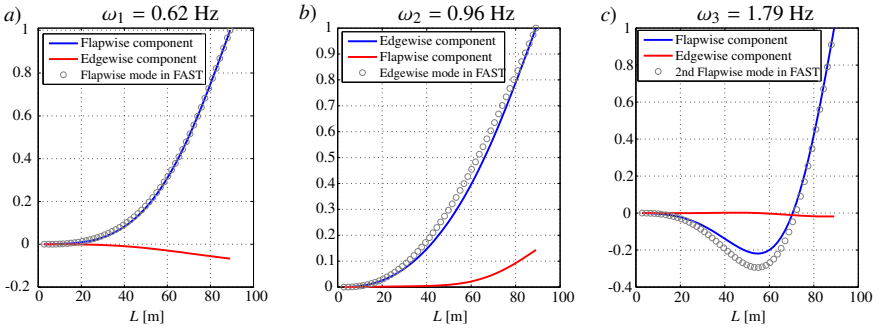

Fig. 5. 3D spacial eigenmodes of a single blade. a) 1st out-of-plane mode. b) 1st in-plane mode. c) 2nd out-of-plane mode.

The first three eigenmodes of a single non-rotating blade is shown in Fig. 5. Due to pre-twist, the eigenmodes become 3D spacial modes rather than 2D planar modes. For example, the 1st out-of-plane mode (Fig. 5a) is dominated by the flap-wise component, but non-zero edgewise component also exists in this mode due to the coupling effect. Similarly, the 1st in-plane mode dominated by edgewise vibration, also contains some flap-wise component (Fig. 5b).

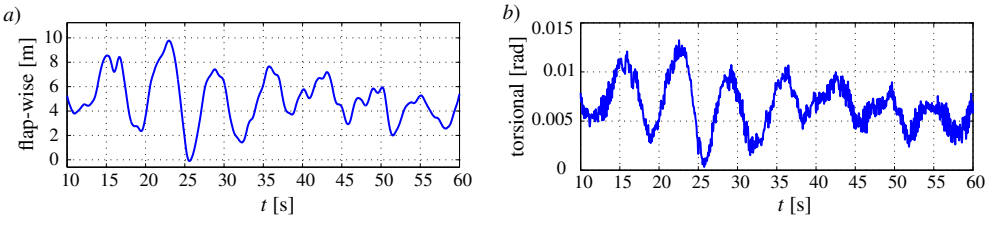

Fig. 6. Blade responses under normal operational conditions (pitch controller on). Ω_0 = 1.0 rad/s, V_0=15 m/s, I=0.1. a) Flap-wise tip displacement. b) Torsional tip deformation (angle).

Fig. 6 shows the time-series of the blade flap-wise tip displacements and torsional tip deformation, when the turbine is under normal operational condition (at nominal rotational speed 1.0 rad/s) with mean wind speed V_0=15 m/s and turbulence intensity I = 0.1. It is seen that the flap-wise vibration is highly damped due to high aerodynamic damping and becomes quasi-static. The torsional vibration is less damped, and eigenvibration is clearly seen in the response.

When the rotational speed of the rotor is gradually increased to 1.6 times the nominal rotational speed, the onset of flutter takes place, which means the critical flutter speed of this 10 MW turbine is $1.6\Omega_0$. Fig. 7 shows the corresponding time-series of the blade responses when $\Omega = 1.6\Omega_0$. It is seen that when flutter takes place, significant negative damping is present in the torsional mode, leading to exponentially increasing amplitude in torsional vibrations.

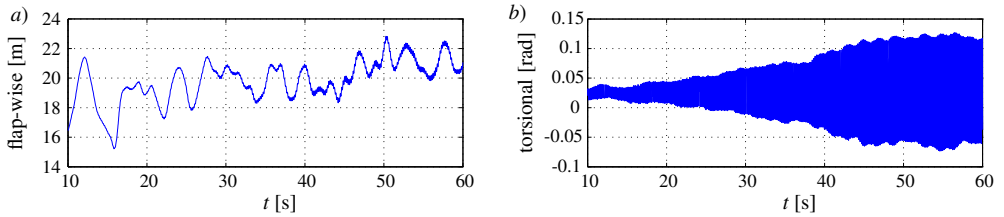

Fig. 7. Flutter response (pitch controller off). $\Omega = 1.6\Omega_0$, V_0=15 m/s, I=0.1. a) Flap-wise tip displacement. b) Torsional tip deformation (angle).

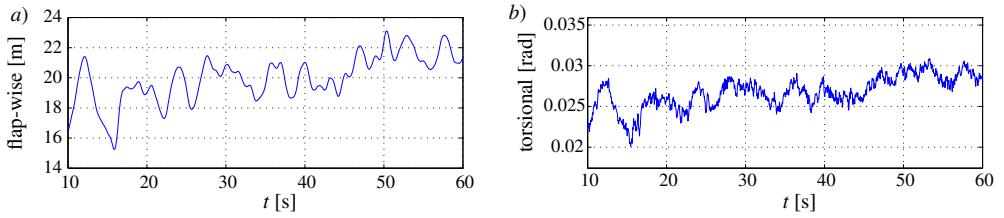

Fig. 8. Blade responses with the damper (pitch controller off). $\Omega = 1.6\Omega_0$, V_0=15 m/s, I=0.1, c_t=421721 Nms, b=48.9 m. a) Flap-wise tip displacement. b) Torsional tip deformation (angle)

To enhance the flutter stability, the proposed torsional viscous damper is installed inside the blade. The design parameters of the damper are the damping constant c_t and the distance b between the fix ends, which need to be optimized during the design phase. Fig. 8 shows the blade responses when the damper ($c_t = 421721$ Nms and $b = 48.9$ m) is mounted, with the same rotor rotational speed $\Omega = 1.6\Omega_0$ as in Fig. 7 (flutter instability in Fig. 7). The torsional damper successfully adds damping into the torsional mode, and flutter no longer takes place when $\Omega = 1.6\Omega_0$. Actually, it is observed that the critical flutter speed is increased to $\Omega = 3.6\Omega_0$ with the damper installed. Therefore, the proposed damper significantly improves the flutter stability of wind turbines.

5. Conclusions

In this paper, a rigorous FE model of the aeroelastic wind turbine system is developed for coupled-mode flutter analysis. The proposed model takes into account all important coupling effects, which are important for accurately carrying out flutter analysis. Simulation results show that the onset of flutter takes place when the rotational speed of the rotor becomes 1.6 times the nominal rotational speed.

Next, a novel electromagnetic torsional viscous damper is proposed to be installed inside the blade, in order to damp torsional vibrations of the blade and to enhance flutter stability of the system. It is shown to be a promising damping device for improving flutter stability of wind turbines, with the potential of being a semi-active device.

References

[1] G. Bir, J. Jonkman, Aeroelastic instabilities of large offshore and onshore wind turbines, Journal of Physics: Conference Series. 75 (2007).
[2] M.H.Hansen, Aeroelastic instability problems for wind turbines, Wind Energy. 10 (2007) 551–577.
[3] S.R. Vatne, Aeroelastic instability and flutter for a 10 MW wind turbine, Master thesis, NTNU, 2011.
[4] D.W. Lobitz, Aeroelastic stability predictions for a MW-sized blade, Wind Energy. 7 (2004) 211–224.
[5] C. Bottasso, F. Campagnolo, A. Croce, C. Tibaldi, Optimization-based study of bend-twist coupled rotor blades for passive and integrated passive/active load alleviation, Wind Energy. 16 (2013) 1149–1166.
[6] C. Bak, F. Zahle, R. Bitsche, T. Kim, A. Yde, L.C. Henriksen, A. Natarajan, M. Hansen, Description of the DTU 10 MW reference wind turbine. DTU Wind Energy Report-I-0092, 2013.
[7] Z. Zhang, S.R.K. Nielsen, F. Blaabjerg, D. Zhou, Dynamics and control of lateral tower vibrations in offshore wind turbines by means of active generator torque, Energies. 7 (2014) 7746–7772.
[8] Z. Zhang, Passive and active vibration control of renewable energy structures. PhD thesis, Aalborg University, Denmark, 2015.
[9] M.O.L. Hansen, Aerodynamics of Wind Turbines, Earthscan, London, 2008.
[10] S. Krenk, M.N. Svendsen, J. Hogsberg, Resonant vibration control of three-bladed wind turbine rotors, AIAA journal. 50(2012) 148–161.
[11] H.A. Sodano, J.S. Bae, Eddy current damping in structures, Shock and Vibration Digest. 36 (2004) 469–478.